Solubilities of a 1,4-Bis(alkylamino)-9,10-anthraquinone Series in Compressed Carbon Dioxide

Cornelia B. Kautz,[‡] Gerhard M. Schneider,[‡] Jae-Jin Shim,[§] Björn Wagner,[||] and Dirk Tuma*[,†]

Applied Thermodynamics, University of Kaiserslautern, D-67653 Kaiserslautern, Germany, Physical Chemistry, University of Bochum, D-44780 Bochum, Germany, School of Display and Chemical Engineering, Yeungnam University, 214-1 Dae-dong, Gyeongsan, Gyeongbuk 712-749, Korea, and Physical Chemistry, Aalen University of Applied Sciences, Beethovenstrasse 1, D-73430 Aalen, Germany

In this work, we report on the solubility of six disubstituted anthraquinone-type disperse dyes in compressed CO_2 between (299 and 346) K and up to a pressure of 20 MPa determined by a flow method. The disperse dyes belong to a series of 1,4-bis(alkylamino)-9,10-anthraquinones, where alkyl = methyl, ethyl, propyl, 1-methylethyl, butyl, pentyl, and octyl. The results of the previously investigated propyl derivative were included for comparative discussion. Significant differences regarding the solubility behavior of the individual dyestuffs were observed under the applied experimental conditions. VIS spectroscopy was applied to determine solubility, and the accessible measuring range was limited by a maximum analyzable solubility of about $450 \cdot 10^{-6}$ mol·dm^{-3}. At any experimental conditions, 1,4-bis(1-methylethylamino)-9,10-anthraquinone with a branched alkyl group shows the highest solubility for that homologous series. For example, at $p = 16.83$ MPa and $T = 310.0$ K, the solubility of 1,4-bis(1-methylethylamino)-9,10-anthraquinone amounted to $s = 418 \cdot 10^{-6}$ mol·dm^{-3} (0.135 g·dm^{-3}). For the dyes substituted with linear alkylamino groups, the solubility passes through a maximum that is observed with 1,4-bis(pentylamino)-9,10-anthraquinone. The solubilities of the methyl and ethyl compound are comparatively low and similar. Equilibrium concentrations of the less-polar propyl- and butyl-substituted derivative are slightly lower than for the pentyl compound, and the sequence of solubility also depends on the experimental conditions. At higher temperatures and pressures, the solubility of the butyl derivative exceeds that of the propyl derivative. Ultimately, the overall solubility again goes down for the octyl compound to values in between those for the methyl- and ethyl-substituted and the propyl- or butyl-substituted compound. Inspired by their prevalent use in the literature, we applied five randomly selected empirical density-based correlations with different numbers of adjustable parameters to our data. Surprisingly, the best performance, i.e., the best agreement between experiment and correlation, for all data sets was observed for the simple concepts, and the introduction of further parameters did not automatically imply a better correlation.

Introduction

During the recent years, our group has been engaged in studying the solubility behavior of the series of 1,4-bis(alkylamino)-9,10-anthraquinone disperse dyes in supercritical fluids, especially carbon dioxide. In addition to their usability as coloring agents in the particular dyeing technique that employs a supercritical fluid as solvent for the solid dyestuff, usually carbon dioxide, a technique that has proven to be successful (see, e.g., Santos et al.,[1] Park and Bae,[2] Hendrix[3]), that kind of anthraquinone derivatives has several advantages which favor their employment in phase equilibrium studies, such as stability on exposure to light and heat, nontoxicity, distinct and thus well analyzable spectral bands, and at least a solubility behavior in carbon dioxide that allows it to cover a remarkably broad p,T region. Therefore, these substances qualify as model substances for systematic solubility investigations to establish fundamentals for subsequent technical applications. Accordingly, a comprehensive data set of equilibrium solubilities of these substances at manifold pressures, temperatures, and solvent gases has been collected and evaluated so far. This work aligns in a series of referring studies. Investigations have begun with a static analytical method,[4−13] later followed by a particularly adapted supercritical fluid chromatography (SFC) device.[6,9,12,14−16]

The present study was elaborated from the doctoral theses of Kautz[17] and Wagner[18] at the University of Bochum. In this paper, each step of the adapted SFC method for measuring equilibrium solubilities is treated equally. It starts with sample preparation, takes a look at spectral characteristics of the investigated dyestuffs, continues with the question how to perform a proper calibration, and ends in the evaluation of the solubility data. New results for the binary systems CO_2 + 1,4-bis(alkylamino)-9,10-anthraquinone, where alkyl = methyl, ethyl, 1-methylethyl, butyl, pentyl, and octyl, that were obtained in the temperature range between (299 and 346) K and pressures up to 20 MPa, respectively, are presented and discussed with regard to our preceding studies. Additionally, the applicability of five commonly used density-based phenomenological models to correlate the solubility data was investigated. We resorted to the following models: the original and well-known concept proposed by Chrastil,[19] an advanced derivative published by

* Corresponding author. Phone: +49 631 205 4114. Fax: +49 631 205 2119. E-mail: tuma@rhrk.uni-kl.de
[†] University of Kaiserslautern.
[‡] University of Bochum.
[§] Yeungnam University.
[||] Aalen University of Applied Sciences.

10.1021/je800252z CCC: $40.75
Published on Web 09/06/2008

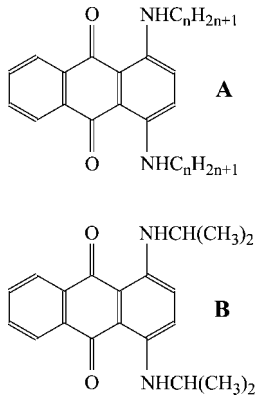

Figure 1. Structures of the anthraquinone dyestuffs: A = 1,4-bis(*normal*-alkylamino)-9,10-anthraquinone, where n = number of carbon atoms in the alkyl chain: $n = 1$ for methyl (AQ01), $n = 2$ for ethyl (AQ02), $n = 3$ for propyl (AQ03), $n = 4$ for butyl (AQ04), $n = 5$ for pentyl (AQ05), $n = 8$ for octyl (AQ08). B = 1,4-bis(1-methylethylamino)-9,10-anthraquinone (AQiso03).

Sung and Shim,[20] that by Clifford and co-workers,[21] that by del Valle and Aguilera,[22] and ultimately that by Méndez-Santiago and Teja.[23]

Experimental

Materials and Preliminary Studies. CO_2 (4.5, volume fraction ≥ 99.995 %) was purchased from Messer Griesheim GmbH, Krefeld, Germany. All organic solvents used during the experiments were of analytical grade and delivered by both J. T. Baker B. V., Deventer, The Netherlands, and Riedel de Haën GmbH & Co. KG, Seelze, Germany. The structures of the anthraquinone dyestuffs are shown in Figure 1. 1,4-Bis(methylamino)-9,10-anthraquinone (abbreviated as AQ01, > 97 %, M = 266.30 g·mol^{-1}, CAS no. 2475-44-7), the ethyl (AQ02, > 98 %, M = 294.35 g·mol^{-1}, CAS no. 6994-46-3), butyl (AQ04, > 98 %, M = 350.46 g·mol^{-1}, CAS no. 17354-14-2), and pentyl (AQ05, > 97 %, M = 378.51 g·mol^{-1}, CAS no. 2646-15-3) derivatives were purchased from Aldrich GmbH, Deisenhofen, Germany, whereas the propyl (AQ03, M = 322.41 g·mol^{-1}, CAS no. 2475-40-3), the 1-methylethyl or isopropyl (AQiso03, M = 322.41 g·mol^{-1}, CAS no. 14233-37-5), a different sample of the butyl (AQ04), and finally the octyl (AQ08, M = 462.67 g·mol^{-1}, CAS no. 86302-54-7) derivatives were synthesized in our laboratories at the University of Bochum. All substances have a similar characteristic blue color. Wagner's work comprised the experiments with AQ01, AQ02, AQ03, AQiso03, and AQ04 purchased from Aldrich and AQ05,[18] and that by Kautz comprised the experiments with AQ04 and AQ08, both substances from domestic synthesis.[17]

The synthesized samples were analyzed by SFC to determine their initial purities. A capillary SFC (HP SFC G1205A, Hewlett-Packard GmbH & Co. KG, Waldbronn, Germany) with CO_2 as the mobile phase and flame ionization detection (FID) was employed. The commercial samples from Aldrich (i.e., AQ01, AQ02, AQ04, and AQ05) were recrystallized from methanol prior to purity analysis. The SFC analyses of these substances and of the laboratory-made AQ03 and AQiso03 were conducted using a SB-cyanopropyl-50 column (Dionex GmbH, Idstein, Germany; length, 10 m; inner diameter, 50 μm) at T = 323 K and p = 20 MPa, whereas for the laboratory-made AQ04 and AQ08, a SB-methyl-100 column (Dionex; length, 10 m; inner diameter, 50 μm) was used. The associated experimental p,T conditions also were slightly different and amounted to T = 343 K and p = 14 MPa for AQ04 and T = 353 K and p = 17 MPa for AQ08, respectively. A purity of > 99 % was found for AQ01, AQ02, AQ03, AQ04 (Aldrich), and AQ05, and AQiso03 had a purity of > 97 %, AQ08 of > 95 %, and AQ04 (laboratory-made) of > 85 % only. All purity data were calculated via peak integration.

A characteristic of the raw material was a reddish tint that was observed for solutions in organic solvents, and that tint was, even more pronounced, unveiled when such a sample dissolved in CO_2.[24] The responsible impurity was identified as an OH-substituted byproduct (1-hydroxy-4-*n*-alkylamino-9,10-anthraquinone) with a significantly better solubility in CO_2 than the actual substance.[18,24] So, the idea was to use a modified SFC for the purification of the substances in a dynamic extraction process, where a CO_2 flow elutes such a byproduct with a better solubility than the genuine substance. However, any byproduct of lower solubility would remain unaffected, but investigations clearly verified the OH-substituted byproduct prevailing.[18,24] The entire procedure was carried out in the same SFC equipment that was employed for solubility measurements (see the following section). The material to be purified was finely pulverized and filled into an extraction column (steel tube; length, 10 cm; inner diameter, 2 mm). Initially, Kautz precipitated both AQ04 (laboratory-made) and AQ08 on silanized kieselguhr (45−70 mesh; Merck KGaA, Darmstadt, Germany) as well on Chromosorb G-AW (60−80 mesh; WGA GmbH, Moers, Germany). Chromosorb G-AM was found to be contaminated with a UV-active impurity, so that it had to be removed under the extraction conditions first. A temperature of 310 K and pressures of approximately 10 MPa proved to be optimum conditions for both effective elution of the byproduct and minimum loss of the sample. Later, Wagner tested extraction columns that were charged with the pure substance without any substrate. This technique proved to be effective as well under the same p,T and flow-rate conditions and was therefore applied for AQ01, AQ03, AQiso03, AQ04 (Aldrich), and AQ05. The diode array detector Polytec X-dap (Polytec GmbH, Waldbronn, Germany) made it possible to monitor the VIS spectra with their characteristic features simultaneously during the purification procedure. After approximately 100 min, the absorption spectrum became equivalent to that of the pure substance, and that period was sufficient for all substances. The analysis with the capillary SFC was repeated after that procedure for each substance, and the refined materials were all of > 99.5 % purity, except AQ08 with > 99.2 % and AQ04 (laboratory-made) with > 97.4 %. These samples became the starting material for calibration as well as solubility measurements. For more details and Supporting Information, the reader is referred to the two theses[17,18] and the paper by Wagner et al.,[24] respectively.

Equipment and Procedures. The apparatus for the dynamic solubility investigations is a modified supercritical fluid chromatograph. It is designed for working temperatures between (25 and 80) °C and up to a maximum pressure of 20 MPa. Figure 2 gives an outline of the experimental device.

The CO_2 from the gas container G is condensed into the working cylinder of a high-pressure syringe pump SP (Isco SFC-500, Isco, Inc., Lincoln, NE, USA) by cooling it to about 277 K with an external cryostat CR (Lauda K4R, Lauda Dr. R. Wobser GmbH & Co. KG, Lauda-Königshofen, Germany). The working cylinder has a volume of 50 mL. During the experiment, the syringe pump operates at constant pressure and enables a pulse-free constant CO_2 flow. The extraction column E, the spectroscopic high-pressure (with a maximum working pressure of 30 MPa) flow-through cell F (cf. Figure 3), and the pressure sensor P (Burster Sensotec Super TJE, Burster GmbH & Co.

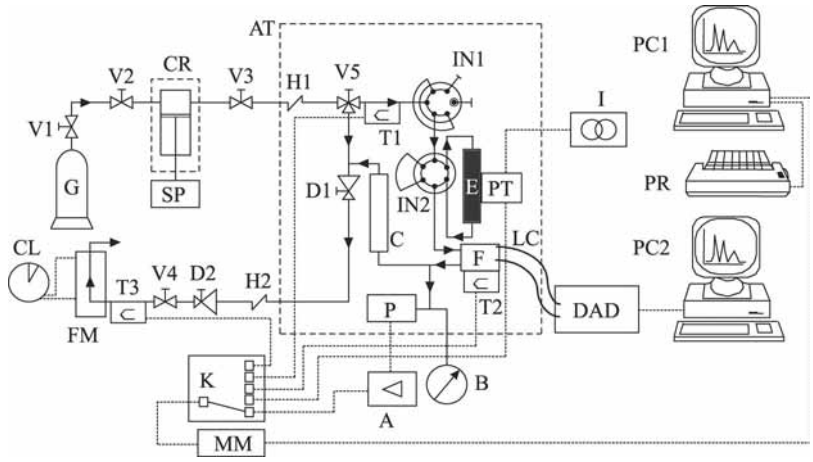

Figure 2. Scheme of the device for solubility investigations. A = amplifier; AT = air thermostat; B = Bourdon gauge; C = column filled with charcoal; CL = electronic time clock; CR = cryostat; D1 = reduction valve; D2 = restrictor valve; DAD = diode array detector; E = extraction column; F = flow-through cell (cf. also Figure 3); FM = flow meter; G = gas container; H1, H2 = heat exchanger; I = current supply; IN1, IN2 = injection valve; K = scanner kit; LC = fiber light conductors; MM = multimeter; P = pressure transducer; PC1, PC2 = computer; PR = printer; PT = platinum resistance thermometer; SP = syringe pump; T1 to T3 = thermocouple; V1 to V5 = valve. − − −, marks a thermostatted area; - - - -, signal wire.

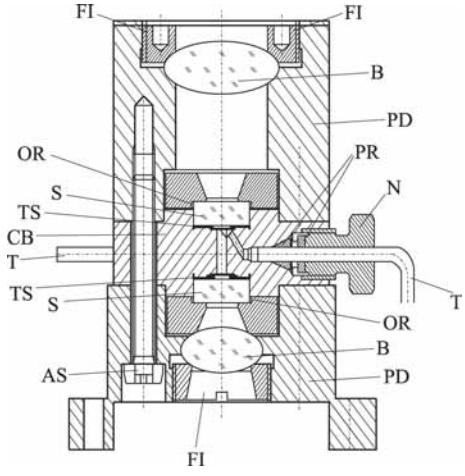

Figure 3. Scheme of the optical high-pressure flow-through cell. AS = adjustment screw; B = biconvex (glass) lens; CB = cell body; FI = fixture; N = nut; OR = O-ring seal; PD = pressure disk; PR = pressure ring; S = sapphire window; T = 1/16 in. capillary tube; TS = Teflon seal.

KG, Gernsbach, Germany) are housed in a custom-made air thermostat AT. The standard tubing of the equipment consists of stainless steel tubes, sized 1/16 in. and with an internal diameter of 0.3 mm. Having entered the air thermostat, the CO_2 passes a heat exchanger coil H1 (stainless steel; length, 2.8 m; internal diameter, 0.2 mm) that is kept at the working temperature. The injection valve IN1 (Rheodyne 7725i, Rheodyne Europe GmbH, Alsbach an der Bergstrasse, Germany) is not used during the solubility experiment, as the CO_2 flow simply passes through. At both ends, the extraction column (stainless steel; length, 20 cm; internal diameter, 2 mm) is closed by (1/16 to 1/8) in. tube fittings with a porous 5 μm metal frit (Swagelok Co., Solon, OH, USA). The fittings are connected with the six-port valve IN2 (Rheodyne 7000). Depending on the valve position, the extraction column that contains the anthraquinone dyestuff can either be bypassed or receive the flowing CO_2. In the bypass position of the valve, the CO_2 pressure inside the column is maintained constant. Afterward, the CO_2 flow, optionally containing dissolved dyestuff, enters the flow-through cell F, which is separately illustrated in more detail in Figure 3. The material of the flow-through cell is stainless steel, and the cell itself was removed from a UV spectrometer (UVIKON 720 LC, Kontron AG, Eching, Germany) and assembled here.

The optical unit consists of two sapphire windows S (BIEG GmbH, Elzach, Germany), each with an additional biconvex lens B. The sample volume amounts to 8 μL, and the optical path length is 5.8 mm. Two fiber light conductors LC (Polytec monofibers; inner diameter, 400 μm) are connected to the flow-through cell by a homemade fixture, which allows for adjusting the fibers to maximum transmission. They link the cell with a diode array detector DAD (Polytec X-dap) that is controlled by a computer PC2. The working pressure p is read via an amplified signal (amplifier A, Burster Semmeg 9000) of the pressure transducer P. An additional Bourdon gauge B (maximum pressure, 36 MPa; Heise Bourdon Tube Co. Inc., Newtown, CT, USA) has been installed to monitor the pressure independently. Ultimately, the CO_2 flow is lead through a column C (stainless steel; length, 8.4 cm; internal diameter, 4 mm), which is filled with charcoal to absorb the dissolved dyestuff before it would precipitate upon the outlet. The mobile phase is expanded in two steps. First, the passage of the reduction valve D1 (type 822/2322, GHR Hochdruck-Reduziertechnik GmbH, Ober-Mörlen, Germany) reduces the pressure from the working pressure to approximately 0.2 MPa at operation temperature. Next, the CO_2 flow is cooled to room temperature in a heat exchanger H2 (copper; size, 1/8 in.; length, 5.9 m) outside the air thermostat. The flow rate can be controlled by the restrictor valve D2 (HBS 300/1; maximum outlet pressure, 1.5 bar; Air Liquide GmbH, Düsseldorf, Germany) and is determined by a soap-film flowmeter FM (SF 11, Horiba/Stec Co., Inc., Kyoto, Japan). The working temperature T (i.e., inside the air thermostat) is recorded at three different spots. One of two thermocouples T1 (type K, Thermocoax GmbH, Stapelfeld, Germany) is embedded in a T-fitting and measures T directly in the CO_2 flow, and the other one (T2) is attached to the flow-through cell. A platinum resistance thermometer PT (type A, JUMO GmbH & Co. KG, Fulda, Germany) is mounted in an aluminum block that is in direct contact with the extraction column and is controlled by a current supply I (model 6424, Burster). The third thermocouple T3 (type K, Thermocoax) records the temperature of the CO_2 flow proximate to the flowmeter. The signals from both the temperature sensors T1 to T3 and the pressure transducer P are collected by a scanner kit K (model 705, Keithley Instruments, Inc., Cleveland, OH,

USA), read by a multimeter MM (model 195A, Keithley), and finally analyzed and processed using the computer PC1.

Any actual equilibrium solubility measurement with a new sample, i.e., another anthraquinone dyestuff, is preceded by the abovementioned purification procedure.

A solubility experiment is carried out as follows. The pulverized and, where appropriate, recrystallized dyestuff is packed into the extraction column that is mounted inside the air thermostat. The syringe pump is loaded with liquid CO_2. The air thermostat with the extraction column is adjusted to the desired working temperature, which is reached as soon as the temperature sensors T1, T2, and T3 give equal and constant values. The working pressure and a constant flow rate of (0.5 to 1.0) mL·s^{-1} referred to $p^\circ = 0.1$ MPa and $T^\circ = 273.15$ K are tuned, while the CO_2 flow is passing the extraction column. Then, the valve IN2 is switched and the column is bypassed for an equilibration time of at least 5 min. A spectrum of the pure CO_2 in the wavelength range between (400 and 750) nm at the respective p,T conditions is recorded as a reference spectrum. Eventually, the extraction column is switched into the CO_2 flow, and spectra (in the visible range) are frequently recorded until no further change in the spectral pattern is observed which indicates equilibrium solubility. During the measurement, temperature T, pressure p, and the flow rate are monitored. After each run, the next working pressure (since the procedure runs isothermal) is adjusted in the extraction column before the CO_2 flow is switched over to bypass the extraction column. The saturation concentrations proved to be independent of the flow rates and equilibration time within the experimental uncertainty.

The calculation of the saturation concentration or equilibrium solubility s resorts to a calibration function that has to be established before. The spectra from calibration experiments are analyzed in exactly the same way as for the solubility measurement by a modified Beer−Lambert law:

$$\int_{\tilde{\nu}_b}^{\tilde{\nu}_e} \log\left(\frac{I_0}{I}\right) d\tilde{\nu} = B_{\tilde{\nu}} cd = A \qquad (1)$$

where A is the "integral absorbance", i.e., the peak area below the spectrum between the two bordering wavenumbers $\tilde{\nu}_b$ and $\tilde{\nu}_e$. $B_{\tilde{\nu}}$ is the molar integrated absorption coefficient for that wavenumber range; d is the optical path length; and c is the concentration, which also can be substituted with the equilibrium solubility s. I and I_0 are the intensities of the sample and the reference signals as a function of wavenumber $\tilde{\nu}$. $B_{\tilde{\nu}}$ is a characteristic constant for an absorbing compound in a selected medium, in our case that of the respective anthraquinone dye in a solvent.

The calibration is performed directly in the flow-through cell at room temperature and atmospheric pressure using different stock solutions of known concentration of the anthraquinone dyestuff in several organic solvents. The flow-through cell is taken out of the air thermostat but still connected with the diode array detector by the fibers. That is done to compensate all systematic errors that are brought in from the cell optics as well as the light conductors and ensures identical conditions for calibration and solubility experiments. The spectrometer records the spectrum within a preset wavelength range and subtracts a buffered baseline (which compensates the characteristics of the pure solvent and the optical parts), and finally the integral absorbance A is calculated as the area between the absorption bands and a baseline that connects the onset and ending of the spectrum (cf. ref 24 for a typical spectrum) at the bottom. The resulting calibration function $A(c)$ is a linear function according to eq 1. Since the Beer−Lambert law is a limiting law, the curve progression can deviate from linearity at higher concentrations and depends also on detector characteristics. In those cases, the calibration points were fitted by a polynomial (see Figure S1 in the Supporting Information). The qualified solvents on the one hand must be able to dissolve such quantities of solid substance so that the weighing error during the solution preparation is kept to a minimum, and on the other hand, the dissolved substance must have a molar integrated absorption coefficient $B_{\tilde{\nu}}$ that is similar (ideally, equivalent) to that in CO_2. For that reason, we also do a calibration directly in CO_2 to validate the results from the calibration in organic solvents.

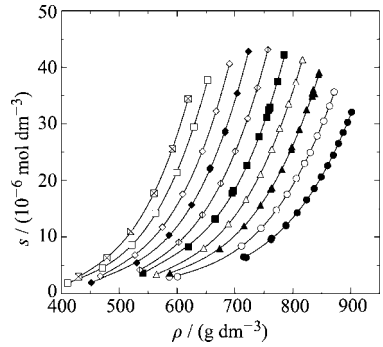

Figure 4. Solubility of AQ01 in CO_2. The solubility s is plotted versus the density ρ of the pure CO_2 at different temperatures T: ●, 299.0 K; ○, 305.0 K; ▲, 310.0 K; Δ, 315.0 K; ■, 320.0 K; diamond with a vertical line, 325.0 K; ♦, 330.0 K; ◇, 335.0 K; □, 340.0 K; square with an x, 345.0 K. Note: The curve here and in the following figures is an eye-guiding polynomial, not a correlation function of any kind.

These particular experiments were carried out in a separate high-pressure autoclave equipped with a movable piston. Here, in contrast to equilibrium solubility measurements, the introduced amount of anthraquinone dyestuff must be completely dissolved at any p,T conditions. Different concentrations are created by changing the cell volume via different pressures. The paper by Wagner et al.[24] provides a detailed report on that experiment.

Experimental Uncertainties. The temperature sensors T1, T2, and T3 were calibrated with a certified ultrahigh-precision platinum resistance thermometer (X2001, XSYS Corp., Sudbury, MA, USA). The uncertainty of the recorded temperatures is below ± 0.01 K. The total uncertainty in the temperature measurement of below ± 0.2 K is estimated from the divergence of the readouts at T1, T2, and T3 that might result from a small temperature gradient.

The pressure transducer P and the Bourdon gauge B were calibrated employing a high-precision pressure balance (model 480D, Budenberg Gauge Co., Ltd., Manchester, UK). The scale-reading accuracy is ± 0.01 MPa for the pressure transducer P and ± 0.05 MPa for the Bourdon gauge B, respectively. Therefore, the maximum uncertainty for the pressure measurement amounts to ± 0.05 MPa (i.e., when referring to the Bourdon gauge). Furthermore, the pressure-induced uncertainty is increased when the solubility isotherms (see Figures 4 to 9) become steeper.

The error that results from the integration of the recorded (VIS) spectra depends on the solute concentration. For concentrations lower than approximately $5 \cdot 10^{-6}$ mol·dm^{-3}, the standard deviation of the peak area calculation can amount to up to ± 5 %, which is noise-induced, whereas at higher concentrations, this contribution levels off, so that for most data this particular contribution is kept below ± 1 %.

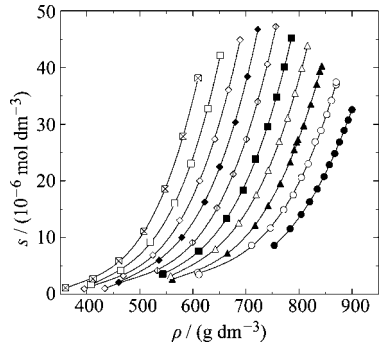

Figure 5. Solubility of AQ02 in CO_2. The solubility s is plotted versus the density ρ of the pure CO_2 at different temperatures T: ●, 299.3 K; ○, 305.0 K; ▲, 310.0 K; Δ, 315.0 K; ■, 320.0 K; diamond with a vertical line, 325.0 K; ♦, 330.0 K; ◇, 335.0 K; □, 340.0 K; square with an x, 346.0 K.

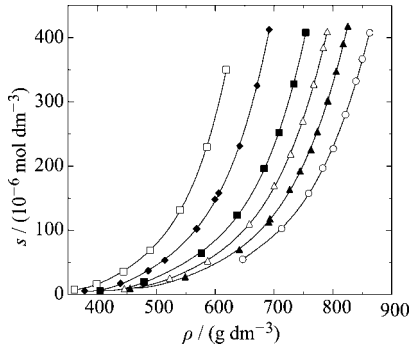

Figure 6. Solubility of AQiso03 in CO_2. The solubility s is plotted versus the density ρ of the pure CO_2 at different temperatures T: ○, 305.0 K; ▲, 310.0 K; Δ, 315.0 K; ■, 320.0 K; ♦, 330.0 K; □, 340.0 K.

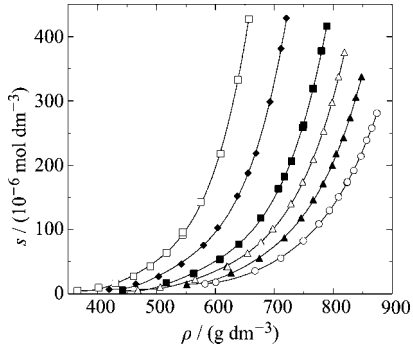

Figure 7. Solubility of AQ04 in CO_2. The solubility s is plotted versus the density ρ of the pure CO_2 at different temperatures T: ○, 305.0 K; ▲, 310.0 K; Δ, 315.0 K; ■, 320.0 K; ♦, 330.0 K; □, 340.0 K. All data illustrated were taken from Wagner's thesis.[18]

The calibration in organic solvents contributes uncertainties from the preparation of the stock solutions and proximate dilution series. The relative error for the determination of the concentration c was normally about (1.5 to 2.0) %. The calibration directly in CO_2 introduces an additional error that results from the volume determination,[24,25] and thus the resulting relative error for c was estimated to be ± (3.5 to 4) %.

Consequently, the maximum relative error of the dyestuff solubility resulting from the temperature measurement was ± 1 %, that from the pressure measurement ± 2.5 %, that from the spectra analysis ± 1 %, that from the calibration in organic solvents between ± (1.5 and 2.0) %, and finally that from the calibration in CO_2 between ± (3.5 and 4.0) %. In a typical experiment, however, those errors can mutually compensate each other, so that a mean relative error of ± 3 % from these particular sources has proven reasonable.

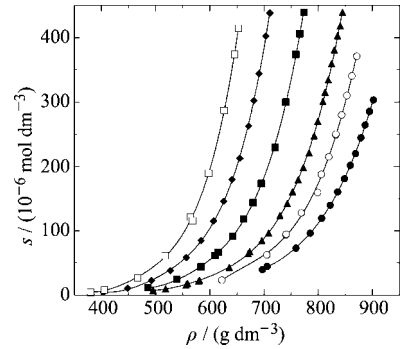

Figure 8. Solubility of AQ05 in CO_2. The solubility s is plotted versus the density ρ of the pure CO_2 at different temperatures T: ●, 299.0 K; ○, 305.0 K; Δ, 310.0 K; ■, 320.0 K; ♦, 330.0 K; □, 340.0 K.

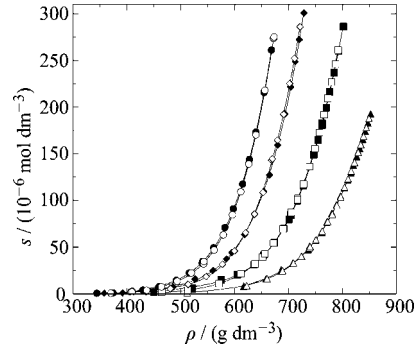

Figure 9. Solubility of AQ08 in CO_2. The solubility s is plotted versus the density ρ of the pure CO_2 at different temperatures T: full symbols = silanized kieselguhr (▲, 310.1 K; ■, 320.0 K; ♦, 329.9 K; ●, 340.1 K); open symbols = Chromosorb G-AW (Δ, 310.3 K; □, 320.0 K; ◇, 330.0 K; ○, 340.1 K).

However, it has to be kept in mind that the following sources of error can by far outreach the errors discussed beforehand. First and most important, if those better-soluble impurities are not sufficiently removed, the results are systematically shifted to higher values, sometimes by a factor of 2 and more. Even if the impurity does not overlap in the wavelength range, the measured equilibrium will become incorrect. This problem is discussed and exemplified in the paper by Wagner et al.[24]

Another important point is the choice of the solvents for calibration. A difference between $B_{\tilde{\nu}}$ of the dyestuff in the organic solvent and that in CO_2 will affect the calibration function which is used for data analysis. Ultimately and without saying, equilibrium conditions must be ensured when recording the absorption spectrum.

Results and Discussion

Calibration. Several different organic solvents were selected for calibration. The calibration directly in CO_2, serving as a cross-check experiment, was done for all anthraquinone dyestuffs except in the earlier studies with the laboratory-made AQ04 and AQ08.[17] The final calibration function to calculate the equilibrium solubility s of the dyestuff in CO_2 from the integrated absorbance A was established in the way that the data for those solvents, where the molar integrated absorption coefficient $B_{\tilde{\nu}}$ of the dyestuff was in accordance with the corresponding CO_2 calibration data, were combined to derive one single linear function. That final function usually included the CO_2 calibration data. The employed solvents and the calibration characteristics are given in Table 1. The original calibration data can be looked up in the respective theses.[17,18]

Table 1. Survey of the Characteristic Parameters for the Calibration[a]

substance	calibration solvent	number of data N_D	concentration range $c/(10^{-6}$ mol·dm$^{-3})$ (and corresponding pressure range p/MPa)	N_D beyond linear behavior ($A > 5600$ cm^{-1}) and $c/(10^{-6}$ mol·dm$^{-3})$ of the first datapoint	molar integrated absorption coefficient $B_{\tilde{\nu}}/(10^{-10}$ cm·mol$^{-1})$
AQ01[b]	acetone	17	$3 \le c \le 125$	—	4.29
	ethanol	15	$1 \le c \le 92$	—	4.40
	heptane	16	$2 \le c \le 73$	—	3.89
	CO_2, $T = 313$ K	4	$31 \le c \le 44$ ($19.5 \le p \le 129.5$)	—	4.32
	CO_2, $T = 333$ K	4	$31 \le c \le 44$ ($28.9 \le p \le 151.0$)	—	
AQ02[b]	acetone	12	$4 \le c \le 74$	—	4.64
	ethanol	13	$2 \le c \le 81$	—	4.70
	heptane	12	$2 \le c \le 71$	—	4.09
	CO_2, $T = 313$ K	4	$29 \le c \le 40$ ($18.3 \le p \le 128.0$)	—	4.83
	CO_2, $T = 333$ K	4	$29 \le c \le 40$ ($28.2 \le p \le 142.0$)	—	
AQ03[b]	acetone	10	$14 \le c \le 392$	4;232	4.59
	ethanol	17	$5 \le c \le 393$	5;251	4.47
	heptane	21	$2 \le c \le 73$	5;250	4.09
	CO_2, $T = 313$ K	8	$31 \le c \le 44$ ($19.5 \le p \le 129.5$)	—	4.29
	CO_2, $T = 333$ K	8	$31 \le c \le 44$ ($28.9 \le p \le 151.0$)	—	
AQiso03[b]	acetone	15	$7 \le c \le 441$	6;275	4.23
	ethanol	10	$6 \le c \le 298$	2;239	4.28
	heptane	23	$4 \le c \le 471$	6;272	3.85
	CO_2, $T = 313$ K	4	$100 \le c \le 138$ ($16.2 \le p \le 95.2$)	—	4.19
AQ04[b] (Aldrich sample)	acetone	16	$7 \le c \le 517$	8;249	4.39
	ethanol	10	$8 \le c \le 342$	2;274	4.48
	heptane	22	$6 \le c \le 482$	8;247	4.12
	CO_2, $T = 313$ K	7	$71 \le c \le 185$ ($28.5 \le p \le 78.6$)	—	4.32
	CO_2, $T = 333$ K	8	$64 \le c \le 182$ ($27.6 \le p \le 97.2$)	—	
	CO_2, $T = 343$ K	4	$128 \le c \le 182$ ($24.5 \le p \le 100.0$)	—	
AQ05[b]	acetone	16	$18 \le c \le 361$	—	4.29
	ethanol	17	$7 \le c \le 372$	—	4.40
	heptane	21	$3 \le c \le 378$	—	3.89
	CO_2, $T = 313$ K	4	$90 \le c \le 126$ ($15.8 \le p \le 100.0$)	—	4.29
	CO_2, $T = 333$ K	4	$90 \le c \le 125$ ($24.7 \le p \le 115.5$)	—	
					$B_\lambda/(10^2$cm^3·mol$^{-1})$
AQ04[c](lab-made sample)	acetone	7	$9 \le c \le 150$	—	1.48
	ethanol	4	$26 \le c \le 260$	—	1.36
	ethyl acetate	8	$56 \le c \le 323$	—	1.31
	1,4-dioxane	12	$7 \le c \le 342$	—	1.35
	heptane	6	$34 \le c \le 138$	—	1.27
AQ08[c]	ethyl acetate	7	$50 \le c \le 187$	—	1.46
	1,4-dioxane	13	$31 \le c \le 246$	—	1.47
	hexane	7	$2 \le c \le 53$	—	1.47
	1-pentanol I	7	$29 \le c \le 262$	—	1.46
	1-pentanol II	5	$85 \le c \le 218$	—	1.49

[a] Those solvents that did not qualify for the final calibration function are indicated in *italic* type. [b] Taken from Wagner's thesis;[18] $d = (0.58 \pm 0.01)$ cm. [c] Taken from Kautz's thesis;[17] $d = (0.58 \pm 0.01)$ cm.

The plot integral absorbance A versus concentration c gives the linear function $A = mc = B_{\tilde{\nu}}cd$, and from the slope m, $B_{\tilde{\nu}}$ can easily be calculated via

$$B_{\tilde{\nu}} = \frac{m}{d} \tag{2}$$

In this study, all spectra of the anthraquinone dyestuffs, without any exception, were recorded between (400 and 750) nm. Initially, the calibration procedure applied by Kautz, which refers specifically to the laboratory-made AQ04 and AQ08,[17] was slightly different. During those experiments, the integral absorbance A was recorded in wavelength units, i.e., nm. The peak analysis itself was done in exactly the same way as for wavenumbers. Thus, $B_{\tilde{\nu}}$ was replaced by B_λ, i.e., the molar integrated absorption coefficient for a wavelength range, only. Later, it was recognized that the wavenumber analysis evidently served better in pinpointing the spectral differences of the calibration solvents. The nonpolar alkanes, such as heptane, had to then be sorted out as calibration solvents for the dyestuffs with shorter alkyl chains (except for AQ08, the reasons were discussed in ref 24), since $B_{\tilde{\nu}}$ was obviously different, and the deviation became pronounced toward higher concentrations. However, in the prior calibration experiments based on wavelengths, those data at higher concentrations which deviated from linearity were discarded. Wagner assigned a peak area of $A = 5600$ cm^{-1} the upper limit for linear behavior of the diode array detector in these systems. A polynomial of degree 3 proved suitable to correlate over the entire concentration range and had to be applied for the highly soluble AQ03, AQiso03, AQ04 (the commercial sample), and AQ05. Figure S1 in the Supporting Information does an exemplary job of visualizing the calibration data for AQ04 (the commercial sample) with both a linear and a nonlinear behavior as well as the deviation found for the nonpolar heptane. As the diode array detector operated reliably and gave repeatable results, we decided for that extension of the calibration (and measurement) range. The polynomial calibration functions were established in such a manner that the complete data for the solute, i.e., over the entire range investigated (cf. Table 1), were drawn on the polynomial. The polynomial calibration functions, however, were only employed to analyze those solubility concentrations with peak areas beyond linear behavior. The supplementary Table S1 provides the calibration functions that were applied for data analysis.

Table 2. Solubility of AQ01 in CO_2

T / K	p / MPa	ρ / (g·dm^{-3})	s / (10^{-6}mol·dm^{-3})	T / K	p / MPa	ρ / (g·dm^{-3})	s / (10^{-6}mol·dm^{-3})
299.0	6.79	715.2	6.47	305.0	7.62	586.6	2.95
	6.86	719.7	6.37		7.66	600.6	2.97
	7.87	762.3	9.56		8.83	711.3	8.38
	7.91	763.6	9.78		9.77	745.2	11.5
	8.85	788.0	12.1		10.83	771.8	14.8
	8.86	788.2	12.0		11.77	790.1	17.6
	9.84	807.6	14.3		12.75	806.2	20.3
	10.85	823.9	16.6		13.75	820.2	23.0
	11.80	837.0	18.6		13.76	820.4	23.0
	12.80	849.1	20.6		14.55	830.2	24.9
	13.80	859.9	22.6		15.60	842.1	27.9
	14.83	870.0	24.5		16.72	853.5	30.5
	15.80	878.7	26.5		17.79	863.4	33.2
	16.79	887.0	28.5		18.73	871.4	35.6
	17.80	894.8	30.3				
	18.74	901.7	32.1				
310.0	8.80	587.7	3.62	315.0	9.81	564.4	3.39
	9.76	673.6	7.94		10.80	645.9	8.01
	10.76	715.7	12.0		11.76	688.7	12.3
	11.76	744.1	15.6		12.75	719.2	16.6
	12.55	761.8	18.5		13.81	744.1	21.1
	12.66	764.0	18.7		14.84	763.8	25.5
	13.60	781.2	21.9		15.67	777.3	29.3
	14.65	797.6	25.4		16.75	792.9	33.6
	14.70	798.3	25.9		17.72	805.2	37.4
	15.65	811.1	29.0		18.72	816.7	41.4
	16.69	823.7	32.5				
	17.58	833.4	34.9				
	17.59	833.5	35.5				
	17.78	835.4	36.0				
	18.00	837.7	35.3				
	18.69	844.4	38.7				
	18.80	845.5	39.1				
320.0	10.72	541.0	3.58	325.0	11.74	535.5	4.16
	11.76	619.6	8.29		12.80	603.0	9.07
	12.79	665.9	13.2		13.75	644.0	13.9
	13.72	695.7	17.8		14.72	675.4	19.5
	13.78	697.3	18.2		15.70	700.5	25.2
	14.70	720.3	22.6		16.72	722.1	31.0
	15.74	741.6	27.8		17.64	738.8	36.4
	16.49	754.8	31.2		18.79	756.9	43.1
	16.70	758.2	32.5				
	16.70	758.2	32.5				
	16.83	760.3	32.8				
	16.84	760.5	33.0				
	17.71	773.5	37.5				
	18.56	785.0	42.2				
330.0	11.70	451.7	1.92	335.0	12.77	467.5	3.07
	12.74	530.4	5.44		13.75	527.1	6.80
	13.75	586.2	10.3		14.74	574.7	11.8
	14.69	624.8	15.7		15.66	609.7	17.6
	15.69	656.7	21.9		16.78	643.8	25.1
	15.71	657.3	22.2		17.74	667.8	32.3
	16.72	683.2	28.5		18.81	690.4	40.6
	16.72	683.2	28.8				
	17.68	703.8	35.4				
	18.74	723.3	42.8				
340.0	12.70	410.8	1.85	345.0	13.79	429.7	2.97
	13.71	470.7	4.48		14.77	478.7	6.31
	14.70	521.8	8.56		15.71	520.2	11.0
	15.65	562.6	14.2		16.77	560.1	17.7
	16.70	599.4	21.4		17.77	591.7	25.6
	17.73	629.1	29.5		18.79	619.2	34.5
	18.69	652.6	37.7				

Solubility Experiments. The solubility measurements were performed at temperatures between (299.0 and 346.0) K and pressures from (6.56 to 19.98) MPa. The solubility isotherms were recorded in intervals of either (5 or 10) K. The corresponding densities of the (pure) CO_2 covering a region from a minimum of 339.6 g·dm^{-3} to a maximum of 901.7 g·dm^{-3} were entirely calculated via the equation of state developed by Span and Wagner[26] which is implemented in the software package ThermoFluids.[27] For the solubility measurements, the laboratory-made AQ04 and the AQ08 were precipitated on a chromatography carrier material, whereas the other dyestuffs were filled directly into the empty column. The dyestuffs most likely remained in the solid state under the experimental conditions. CO_2-induced melting point depression is known from the literature[28,29] and was also observed as a side effect during earlier experiments with disperse dyestuffs.[30] For AQ05, the

Table 3. Solubility of AQ02 in CO_2

T / K	p / MPa	ρ / (g·dm^{-3})	s / (10^{-6}mol·dm^{-3})	T / K	p / MPa	ρ / (g·dm^{-3})	s / (10^{-6}mol·dm^{-3})
299.3	7.72	753.3	8.62	305.0	7.69	608.8	3.83
	8.78	783.3	11.6		7.70	611.3	3.49
	9.79	804.0	14.1		8.81	710.4	8.64
	10.74	819.9	16.3		9.81	746.3	11.7
	11.75	834.2	18.6		10.79	770.9	14.9
	12.81	847.3	20.8		11.71	789.1	17.5
	13.72	857.3	22.9		12.63	804.3	20.6
	14.71	867.1	24.8		13.52	817.2	23.0
	15.70	876.2	26.9		14.55	830.2	26.9
	16.74	885.0	28.9		15.52	841.2	28.9
	17.70	892.5	30.8		16.60	852.3	31.7
	18.69	899.8	32.6		17.53	861.0	34.2
					18.56	870.0	37.0
					18.56	870.0	37.4
310.0	8.66	560.9	2.65	315.0	9.76	558.0	3.25
	9.61	665.0	7.25		10.74	642.5	8.00
	10.80	717.0	12.2		11.70	686.5	12.6
	11.67	741.9	15.7		12.75	719.2	17.5
	12.70	764.8	19.5		13.70	741.8	21.9
	13.74	783.6	23.4		14.77	762.5	27.0
	14.20	790.9	25.5		15.74	778.4	31.1
	14.51	795.6	26.9		16.72	792.4	35.5
	14.69	798.2	27.3		17.74	805.4	39.9
	15.50	809.2	29.8		18.66	816.0	43.9
	16.59	822.5	33.5				
	17.58	833.4	37.1				
	18.14	839.1	39.4				
	18.54	843.0	40.3				
320.0	10.74	543.0	3.55	325.0	10.70	434.0	1.03
	11.61	611.0	7.59		11.71	533.1	4.19
	12.72	663.3	13.3		12.72	598.9	9.11
	13.69	694.8	18.4		13.79	645.5	15.2
	14.59	717.8	23.8		14.74	675.9	21.2
	14.60	718.0	24.0		15.70	700.5	27.4
	15.69	740.6	29.6		16.73	722.3	34.0
	16.68	757.9	34.8		17.74	740.5	40.6
	17.64	772.5	40.1		18.75	756.3	47.2
	18.59	785.4	45.2				
330.0	11.80	460.2	2.10	335.0	11.75	395.2	0.96
	12.83	536.1	6.00		12.79	468.8	3.25
	13.60	579.0	10.0		13.70	524.4	6.91
	14.61	621.9	16.3		14.75	575.2	13.0
	15.45	649.7	22.5		15.75	612.8	20.0
	15.48	650.6	22.5		16.69	641.3	27.4
	16.59	680.1	30.3		17.71	667.1	36.1
	17.63	702.8	38.4		18.73	688.9	44.9
	18.68	722.3	46.8				
340.0	12.65	407.7	1.70	346.0	12.60	359.8	1.13
	13.59	463.9	4.18		13.59	411.4	2.74
	14.65	519.5	9.23		14.56	460.2	5.88
	15.73	565.6	16.1		15.62	508.0	11.1
	16.60	596.2	23.1		16.65	547.8	18.6
	17.69	628.1	32.7		17.69	581.7	27.9
	18.63	651.2	42.2		18.69	609.5	38.1

difference between melting point (T_{fus} = 389 K)[9] and 340 K, the highest temperature during the solubility experiments, amounts to 49 K. In the case of the column being filled with the dyestuff only, column bleeding may be expected when the substance transforms into the liquid state. However, since there is not more than a 10 K difference for AQ08 (T_{fus} = 349 K),[9] AQ08 is probably liquid under elevated CO_2 pressure at that experimental temperature (340.1 K), but the substance was precipitated on carrier material for our experiments. Furthermore, for AQ01, AQ02, and AQ05, the isotherm recorded at 299 K is below the critical temperature ($T_c(CO_2)$ = 304.1 K).[27]

In some earlier papers on that subject, we resorted to selected solubility data, but so far mostly in a different context. Exceptionally, the entire solubility data for AQ03 in CO_2 were reported in the paper by Wagner et al.,[15] and an incomplete selection of data for AQ01 can be drawn from the paper by Kautz et al.[14] The solubility data discussed in the other papers were given in diagrams without data tables, only with reference to the two doctoral theses.[17,18] Only particular aspects of the experiment were highlighted therein. Those papers, among other things, discussed the influence of alkyl chain length on the solubility[9,14] and the energetic aspects of the solution process,[31] compared the results with those obtained from different methods,[6] and dealt with modeling the solubility behavior using an equation of state.[16] Prior to this work, the data sets were provided to the making of the reference data manual entitled "Solubility in Supercritical Carbon Dioxide" edited by Gupta and Shim.[32] That book displays our entire solubility data as isotherm mole fraction solubility versus pressure. All data in that manual are the original data from the two theses, except

for AQ05, where a new refined calibration function (cf. Table S1) was applied to calculate the solubility that is given in this work. The adapted equations to calculate the equilibrium solubility s from the peak areas A recorded during the experiment are

$$s/10^{-6}\ \text{mol·dm}^{-3} = a(A/\text{cm}^{-1}) \quad (3)$$

$$s/10^{-6}\ \text{mol·dm}^{-3} = b(A/\text{cm}^{-1})^3 + c(A/\text{cm}^{-1})^2 + d(A/\text{cm}^{-1}) \quad (4)$$

The coefficients a, b, c, and d are given in the Supporting Information, too.

Tables 2 to 7 give the solubility data for AQ01, AQ02, AQiso03, AQ04, AQ05, and AQ08 in CO_2. The solubility is reported as amount-of-substance (equilibrium) concentration s, obtained by application of eqs 3 and 4, and Figures 4 to 9 illustrate the corresponding solubility behavior in a plot solubility s versus the density ρ of pure CO_2 for all investigated systems.

The maximum solubility value was recorded during the investigation of AQ05 at $p = 18.75$ MPa for $T = 310.0$ K and amounted to $439.2 \cdot 10^{-6}$ mol·dm^{-3} or 0.166 g·dm^{-3}. Due to such low absolute solubilities, the fluid phase can be regarded as an infinitely dilute solution, and thus it is allowed to consider the CO_2 phase as pure. Intrusion of CO_2 into the solid (or perhaps liquid) dyestuff is also neglected. Therefore, if the solubility s_2 (1 = solvent, i.e., CO_2, 2 = low-volatility solute, i.e., disperse dyestuff) shall be given as mole fraction x_2, the following relations can be applied, where x_1 and x_2 are the mole fractions of the two components; V_{mix} is the volume of the saturated CO_2 phase; $V^*_{m,1}$ and $V^*_{m,2}$ are the molar volumes of the pure components; and V^E_m is the excess volume

$$s_2 = \frac{x_2}{V_{mix}} \quad \text{with} \quad V_{mix} = x_1 V^*_{m,1} + x_2 V^*_{m,2} + V^E_m \quad (5)$$

Because of the low saturation concentration of the dyestuff in those binary systems, $x_2 \ll x_1$ and V^E_m is neglected, which simplifies V_{mix} to

$$V_{mix} \approx V^*_{m,1} \quad (6)$$

and

$$x_2 = \frac{s_2 M_1}{\rho_1} \quad (7)$$

As can be seen in Figures 4 to 9, at a constant temperature the solubility monotonously increases toward higher solvent densities for all binary systems. At a constant density, the solubility increases with increasing temperatures which is characteristic for an endothermal solution process. Furthermore, the solubility also monotonously increases with increasing pressure at a constant temperature. Such plots of solubility s versus pressure p are given in the aforementioned papers.[6,9,14−16,31] Here, in contrast to the density plot, the ascent of the isotherms changes with different temperatures, and there exists a "crossover pressure".[33] Below that pressure, increasing temperatures at a constant pressure lead to decreasing solubility, whereas at pressures higher than the crossover pressure the solubility behavior reverts. The explanation for this phenomenon is two competing effects, namely, the temperature-induced increase of the vapor (or sublimation) pressure of the solute and the density behavior of the solvent. Toward higher temperatures, the density decreases. Below the crossover pressure, the density effect manifests stronger, whereas at higher pressures the vapor pressure effect dominates.

Table 4. Solubility of AQiso03 in CO_2

T/K	p/MPa	ρ/(g·dm^{-3})	s/(10^{-6}mol·dm^{-3})	T/K	p/MPa	ρ/(g·dm^{-3})	s/(10^{-6}mol·dm^{-3})
305.0	7.91	646.6	55.0	310.0	8.36	455.2	9.94
	8.86	712.6	102.6		8.61	548.8	27.9
	10.26	758.5	157.5		9.27	641.0	70.3
	11.36	782.6	196.8		10.11	690.8	113.1
	12.39	800.6	227.0		10.16	693.0	118.2
	13.84	821.4	279.8		11.10	726.4	163.7
	15.33	839.2	332.1		11.76	744.1	192.6
	16.34	849.7	366.5		12.59	762.6	225.7
	17.71	862.6	407.3		13.17	773.7	253.8
					14.20	790.9	301.0
					14.22	791.2	302.5
					15.24	805.8	347.5
					16.17	817.6	390.2
					16.83	825.2	417.7
315.0	9.16	445.5	9.33	320.0	9.71	404.5	6.10
	9.53	522.7	25.8		10.21	478.8	19.8
	10.01	587.0	52.8		11.11	576.4	64.7
	11.03	658.0	110.2		12.10	637.1	123.8
	12.10	700.3	169.5		13.30	683.2	196.2
	13.10	728.1	219.1		14.20	708.4	252.1
	14.05	749.0	270.8		15.33	733.6	327.8
	15.05	767.4	327.5		16.42	753.6	407.8
	16.09	783.6	384.5				
	16.57	790.4	409.4				
330.0	10.85	377.7	5.72	340.0	11.88	360.5	7.72
	11.55	438.8	17.6		12.50	398.5	17.2
	12.12	486.1	37.3		13.25	444.1	35.7
	12.50	514.2	53.6		14.05	489.3	68.8
	13.39	568.4	102.3		15.10	539.9	131.8
	14.05	599.7	148.2		16.29	585.9	229.6
	14.20	606.0	158.0		17.35	618.8	349.8
	15.19	641.7	231.1				
	16.22	671.0	325.1				
	17.10	691.7	412.2				

Table 5. Solubility of AQ04 in CO_2

T	p	ρ	s	T	p	ρ	s	T	p	ρ	s	T	p	ρ	s
K	MPa	($g \cdot dm^{-3}$)	($10^{-6} mol \cdot dm^{-3}$)	K	MPa	($g \cdot dm^{-3}$)	($10^{-6} mol \cdot dm^{-3}$)	K	MPa	($g \cdot dm^{-3}$)	($10^{-6} mol \cdot dm^{-3}$)	K	MPa	($g \cdot dm^{-3}$)	($10^{-6} mol \cdot dm^{-3}$)
305.0[a]	7.61	582.3	15.7	310.0[a]	8.62	551.4	15.1	310.1[b]	8.42	474.8	2.2	320.0[b]	9.48	371.5	1.2
	7.66	600.6	18.3		9.11	626.6	32.9		8.72	569.0	13.4		9.98	445.3	4.7
	8.11	667.2	35.9		9.78	674.7	55.5		8.90	599.0	21.9		10.00	448.3	4.2
	8.82	710.8	55.6		10.80	717.0	87.1		8.97	608.2	25.5		10.27	487.1	9.2
	9.91	749.2	82.6		11.81	745.4	118.4		9.16	628.8	34.7		10.50	516.5	14.9
	11.00	775.4	108.8		12.75	765.8	146.3		9.50	655.9	48.8		10.70	538.9	20.7
	11.01	775.6	108.8		13.70	782.9	171.6		9.73	670.2	57.9		11.04	570.7	33.7
	11.96	793.5	129.7		14.70	798.3	199.9		9.97	682.7	73.7		11.29	590.0	44.3
	12.94	809.0	150.7		15.17	804.9	217.9		10.48	704.5	93.8		11.52	605.4	54.7
	14.00	823.5	173.3		16.17	817.6	242.7		10.99	721.9	114.5		12.03	633.7	78.1
	14.04	824.0	174.2		17.13	828.6	274.0		11.53	737.3	135.2		12.49	654.3	102.7
	14.94	834.8	191.7		18.08	838.5	305.6		12.01	749.1	153.6		12.54	656.3	105.5
	16.07	847.0	214.1		19.08	848.1	337.6		12.59	761.7	175.8		13.13	677.7	135.7
	17.04	856.5	238.9						13.04	770.5	192.2		13.35	684.8	158.9
	18.04	865.5	257.9						13.54	779.4	210.5		13.58	691.7	158.3
	19.06	874.1	280.9						13.61	780.6	212.7		14.00	703.3	182.7
315.0[a]	9.26	468.4	6.41	320.0[a]	9.96	442.3	5.89		14.02	787.3	226.2		14.50	715.7	206.3
	9.44	506.1	11.0		10.50	516.5	17.4		14.54	795.3	244.4		14.53	716.4	222.9
	9.82	565.7	22.8		10.95	563.0	31.9		15.07	802.8	262.2		14.95	725.8	227.0
	10.38	619.0	42.9		10.96	563.9	32.0		15.57	809.5	277.4		15.08	728.5	253.5
	10.40	620.5	42.6		11.55	607.3	53.7		16.10	816.1	293.6		15.56	738.2	278.4
	10.96	654.5	63.4		12.15	639.4	77.2		16.65	822.6	309.6		16.05	747.2	304.3
	11.46	677.2	81.0		13.10	676.7	118.0		17.13	828.0	322.6		16.51	755.1	325.2
	12.00	697.0	101.5		14.14	706.9	163.6		17.65	833.5	336.1		17.07	764.1	350.5
	12.01	697.3	101.6		14.55	716.8	182.1		18.26	839.7	350.8				
	13.10	728.1	140.6		15.10	728.9	206.2	330.1[b]	10.40	339.6	1.1	340.1[b]	11.97	365.2	4.2
	14.00	748.0	174.0		16.11	748.3	258.4		10.91	381.7	2.8		12.44	393.9	7.4
	15.00	766.5	209.1		16.19	749.7	262.7		11.40	424.4	6.3		12.99	427.6	14.1
	16.10	783.8	253.1		17.18	765.8	319.1		11.91	467.8	13.8		13.49	457.2	23.6
	17.14	798.0	297.8		18.19	780.2	377.7		12.24	493.8	20.9		13.92	481.3	35.2
	18.04	809.0	337.7		18.87	789.0	416.4		12.50	512.8	28.5		14.53	512.7	59.0
	18.94	819.1	375.6						12.97	543.4	47.6		15.07	537.7	86.3
330.0[a]	11.33	419.6	7.10	340.0[a]	11.97	366.0	4.88		13.33	563.9	63.7		15.58	558.9	120.5
	11.86	465.1	15.4		12.55	401.6	9.86		13.67	581.2	81.1		16.10	578.4	156.9
	12.35	503.4	27.2		13.02	430.3	16.6		14.05	598.5	102.6		16.60	595.3	198.3
	12.93	542.3	46.4		13.54	461.1	27.4		14.10	600.7	104.8		17.16	612.5	246.8
	13.62	580.0	75.5		14.05	489.3	42.7		14.25	606.9	115.2		17.62	624.6	288.5
	14.15	603.9	102.9		14.60	517.1	64.1		14.59	620.1	137.3		17.80	630.2	311.4
	15.05	637.2	151.9		15.20	544.2	91.5		14.96	633.2	159.9				
	15.64	655.3	187.6		15.20	544.2	95.7		15.46	649.1	195.1				
	16.14	668.9	218.7		15.99	575.3	142.8		15.54	651.5	202.8				
	17.14	692.6	298.2		17.00	608.6	217.9		15.98	663.8	230.6				
	18.06	711.1	381.2		18.09	638.3	332.8		16.01	664.6	237.5				
	18.59	720.7	428.6		18.86	656.4	427.1		16.46	676.1	263.2				
									16.56	678.6	278.8				
									16.97	688.1	294.7				
									17.08	690.5	314.6				
									17.57	700.9	347.7				

[a] Filled directly into the extraction column; cf. Wagner's thesis.[18] [b] Precipitated on silanized kieselguhr; cf. Kautz's thesis.[17]

Table 6. Solubility of AQ05 in CO_2

T/K	p/MPa	ρ/(g·dm^{-3})	s/(10^{-6}mol·dm^{-3})	T/K	p/MPa	ρ/(g·dm^{-3})	s/(10^{-6}mol·dm^{-3})
299.0	6.56	697.0	39.7	305.0	7.75	622.1	23.3
	6.66	705.7	44.5		8.70	705.2	62.5
	7.76	758.8	72.9		9.61	740.3	93.5
	8.72	785.0	96.1		9.63	741.0	94.5
	9.76	806.2	119.3		10.70	768.9	127.7
	10.72	822.0	139.6		11.75	798.8	159.4
	11.69	835.6	160.3		12.72	805.7	187.6
	12.72	848.2	180.7		13.70	819.6	214.7
	13.74	859.3	201.6		14.72	832.2	248.3
	14.70	868.8	219.8		14.74	832.5	250.0
	15.78	878.6	244.3		15.70	843.2	279.8
	16.74	886.6	264.1		16.64	852.7	310.1
	17.74	894.4	285.3		17.64	862.0	340.4
	18.74	901.7	303.1		18.69	871.1	371.0
310.0	8.45	495.4	7.27	320.0	10.26	485.7	11.2
	8.51	518.4	9.72		10.70	538.9	24.2
	8.64	556.3	16.0		11.20	583.4	43.7
	8.65	558.7	18.1		11.59	609.7	61.3
	8.75	579.1	21.4		11.69	615.6	66.5
	8.76	580.9	23.1		12.21	642.2	91.3
	9.21	635.9	43.1		12.70	662.5	118.1
	9.71	670.8	64.2		13.20	680.0	143.5
	9.76	673.6	67.8		13.69	694.8	173.0
	10.23	696.0	84.9		14.70	720.3	229.2
	10.55	708.4	96.7		15.68	740.4	299.7
	11.20	729.3	123.7		15.69	740.6	299.8
	11.71	742.9	142.4		16.72	758.6	373.8
	12.12	752.6	160.6		17.19	765.9	405.9
	12.60	762.8	179.0		17.69	773.2	439.1
	13.11	772.6	198.2				
	13.71	783.1	220.8				
	14.30	792.4	247.5				
	14.75	799.0	269.7				
	15.44	808.4	301.0				
	15.75	812.4	315.1				
	16.24	818.4	334.4				
	16.77	824.6	359.4				
	17.24	829.8	380.9				
	17.79	835.5	402.8				
	18.28	840.5	418.4				
	18.75	845.0	439.2				
330.0	11.15	403.8	4.34	340.0	12.20	380.0	4.37
	11.66	448.3	10.6		12.61	405.3	8.07
	12.20	492.2	22.5		13.64	466.8	26.6
	12.69	527.1	38.0		14.61	517.6	61.2
	13.17	556.4	58.2		15.69	564.1	121.2
	13.70	583.9	84.6		15.79	567.9	115.7
	14.22	606.8	115.2		16.64	597.5	188.9
	14.70	625.1	145.8		17.63	626.5	286.8
	15.17	641.0	179.4		18.39	645.6	373.9
	15.65	655.6	212.5		18.69	652.6	414.4
	16.23	671.2	262.3				
	16.64	681.3	301.8				
	17.05	690.6	344.3				
	17.65	703.2	402.3				
	18.04	710.8	438.1				

Looking at the structures of the dyestuffs, particularly on the relation between alkyl chain length and solubility in CO_2, there is no regularity found. The solubilities of AQ01 and AQ02 are low and rather similar, followed by a significant solubility increase for AQ03, AQiso03, AQ04, and AQ05. The AQiso03 with its branched substituents is the best soluble dyestuff at all p,T conditions of our experiments, and AQ05 shows the highest solubility for the linear alkyl chains. However, the solubility decreases again when the alkyl chain is elongated linearly (cf. AQ08). It is still an open question which dyestuff the best solubility is associated with. Therefore, we are planning to investigate the missing AQ06 and AQ07 as well. The influence of substituents, the characteristics of the solid state, and the effect of other solvents (i.e., solvent gases) on the solubility were discussed in detail in a preceding publication.[9]

At present, there are no literature data available for AQ02, AQ03, and AQ05. In the initial stage of our project, analogous solubility experiments for AQ01, AQ04, and AQ08 were done employing a static analytical method and followed by a paper.[5]

Solubility isotherms of AQ01 in CO_2 were also investigated by Joung and Yoo {at (313.15, 353.15, and 393.15) K and pressures of (10, 15, 20, and 25) MPa}[34] and by Gordillo et al. at (313, 333, and 353) K and pressures between (10 and 35) MPa[35] in two similar flow-type devices equipped with an equilibration autoclave. The course of the isotherms published by Joung and Yoo is similar to ours, but the data from Gordillo

Table 7. Solubility of AQ08 in CO_2

T	p	ρ	s	T	p	ρ	s	T	p	ρ	s	T	p	ρ	s
K	MPa	($g \cdot dm^{-3}$)	($10^{-6} mol \cdot dm^{-3}$)	K	MPa	($g \cdot dm^{-3}$)	($10^{-6} mol \cdot dm^{-3}$)	K	MPa	($g \cdot dm^{-3}$)	($10^{-6} mol \cdot dm^{-3}$)	K	MPa	($g \cdot dm^{-3}$)	($10^{-6} mol \cdot dm^{-3}$)
310.1[a]	9.04	616.4	7.9	320.0[a]	10.01	449.8	1.6	310.3[b]	8.53	504.6	0.9	320.0[b]	10.11	464.5	1.5
	9.04	616.4	8.1		10.54	521.2	6.2		9.12	619.4	8.8		10.47	512.9	3.7
	9.54	658.6	16.4		11.09	574.8	15.1		9.59	657.9	16.1		11.04	570.7	11.0
	9.55	659.3	16.2		11.51	604.8	20.4		10.13	687.2	24.7		11.62	611.5	21.5
	10.01	684.7	25.5		12.06	635.2	31.1		10.64	707.8	32.8		12.11	637.6	32.0
	10.03	685.6	24.1		12.47	653.4	41.4		11.08	722.3	40.1		12.44	652.2	39.3
	10.03	685.6	24.6		13.01	673.7	55.0		11.61	737.3	49.4		12.53	655.9	42.9
	10.57	707.8	33.0		13.55	690.8	69.8		11.71	739.9	50.5		12.97	672.3	54.5
	11.06	724.0	40.2		13.92	701.1	79.8		12.11	749.5	58.1		13.50	689.3	69.6
	11.50	736.5	47.4		14.02	703.8	84.3		12.65	761.2	67.3		14.05	704.6	87.1
	11.60	739.1	51.0		14.52	716.1	99.8		13.20	771.8	77.3		14.53	716.4	102.1
	11.60	739.1	51.4		15.02	727.3	115.6		13.68	780.2	85.6		14.54	716.6	100.8
	12.06	750.3	57.1		16.02	746.7	148.9		13.72	780.9	85.1		15.03	727.5	117.4
	12.59	761.7	65.8		16.48	754.6	164.7		14.20	788.7	94.9		15.58	738.5	136.0
	13.07	771.1	77.0		16.95	762.2	180.6		14.69	796.1	103.9		16.14	748.8	155.5
	13.56	779.8	86.0		16.99	762.8	182.8		15.23	803.6	114.1		16.63	757.1	172.8
	14.07	788.1	95.3		17.45	769.8	199.2		15.74	810.3	123.1		17.16	765.4	191.8
	14.60	796.2	104.6		17.95	776.9	216.4		16.18	815.8	131.4		17.65	772.7	209.4
	15.08	803.0	113.4		18.53	784.6	237.1		16.70	821.9	140.5		18.13	779.4	226.8
	15.57	809.5	122.2		19.19	792.9	260.0		16.71	822.1	140.6		18.68	786.6	246.0
	16.01	815.0	129.6		19.98	802.1	286.3		17.31	828.7	151.9		19.11	791.9	261.1
	16.44	820.2	137.7						17.34	829.1	151.6				
	16.98	826.1	146.8						17.79	833.8	159.9				
	17.48	831.7	155.7						18.29	838.9	168.8				
	18.02	837.3	165.5						18.82	844.0	178.1				
	18.51	842.2	174.1						19.35	848.9	187.9				
	19.03	847.1	183.0					330.0[b]	11.53	437.1	2.0	340.1[b]	12.05	370.1	0.7
	19.58	852.1	192.4						12.05	480.5	5.5		12.66	407.5	2.0
329.9[a]	10.60	357.7	0.6	340.1[a]	11.62	344.3	0.6		12.49	513.5	10.1		12.69	409.3	2.0
	11.00	391.9	1.0		12.12	374.3	1.1		12.49	513.5	10.2		13.14	436.6	3.9
	11.51	436.8	2.9		12.70	409.9	2.5		13.01	547.1	18.6		13.61	464.1	7.5
	12.09	485.2	7.3		13.02	429.4	4.1		13.56	577.1	31.7		14.14	493.0	13.5
	12.66	526.5	15.7		13.52	458.9	7.6		14.05	599.7	46.0		14.67	519.4	22.4
	13.20	559.4	25.0		14.11	491.4	14.4		14.59	621.1	65.5		15.15	541.1	31.9
	13.69	584.6	37.3		14.59	515.6	22.4		15.07	637.8	85.5		15.19	542.9	34.6
	13.91	594.7	44.2		15.11	539.4	32.9		15.57	653.3	108.6		15.65	561.6	46.8
	14.48	618.1	63.3		15.13	540.3	34.7		16.11	668.1	143.3		16.11	578.7	63.1
	15.01	636.8	85.1		15.63	560.9	49.3		16.17	669.7	144.6		16.61	595.7	84.6
	15.56	653.9	109.7		16.19	581.6	70.9		16.55	679.2	164.6		17.11	611.1	109.3
	15.93	664.2	127.2		16.66	597.3	91.1		17.05	690.6	192.4		17.64	626.0	139.0
	16.54	679.7	159.4		17.23	614.6	117.5		17.62	702.6	225.2		18.16	639.3	170.2
	17.13	693.2	192.7		17.72	628.1	143.9		18.08	711.5	252.3		18.87	655.9	218.0
	17.63	703.5	221.6		18.19	640.1	173.3		18.65	721.8	286.1		19.64	672.0	273.6
	18.09	712.4	248.6		18.82	654.8	215.6						19.68	672.8	275.1
	18.50	719.9	272.2		19.48	668.8	261.1								
	19.01	728.5	300.9												

[a] Precipitated on silanized kieselguhr; cf. Kautz's thesis.[17] [b] Precipitated on Chromosorb G-AW; cf. Kautz's thesis.[17]

et al. deviate considerably, especially for lower pressures (cf. Figure S2 in the Supporting Information). For example, the $s(\rho)$-isotherm at $T = 313$ K starts with higher values than found by us, and a flat ascent at lower densities turns into a rather steep ascent at higher densities. If we compare the 313 K isotherm from Joung and Yoo to our isotherm at $T = 315.0$ K, Joung and Yoo report lower solubilities (even below our isotherm at $T = 310.0$ K) over the entire range. A polynomial regression for our isotherm at $T = 315.0$ K yields $s = (4.33 \cdot 10^{-6}$, $26.4 \cdot 10^{-6}$, and $46.4 \cdot 10^{-6})$ mol·dm^{-3} for $p = (10$, 15, and 20) MPa, respectively. The corresponding data from Joung and Yoo at $T = 313.15$ K are $s = (3.34 \cdot 10^{-6}$, $14.1 \cdot 10^{-6}$, and $25.6 \cdot 10^{-6})$ mol·dm^{-3} at $p = (10$, 15, and 20) MPa, respectively,[34] and from Gordillo et al. at $T = 313$ K are $s = (12.1 \cdot 10^{-6}$, $20.5 \cdot 10^{-6}$, and $24.1 \cdot 10^{-6})$ mol·dm^{-3} for $p = (10$, 15, and 20) MPa, respectively.[35] Note that Gordillo et al. did not provide any data tables in their paper. Thus, we resorted to the reference data manual edited by Gupta and Shim,[32] who extracted the corresponding numerical values for the measured solubilities by digitizing the graphs. Looking at our prior results from the static method,[5] those data are systematically shifted to higher values at all p,T conditions investigated. The corresponding data table for the diagrams in the respective paper[5] is given in the Supporting Information for comparison. As already mentioned, we could later prove (cf. subsection Materials and Preliminary Studies) that better-soluble impurities were responsible for deviations. At $p = 15$ MPa, for example, the relative deviation between the result from the static method and the corresponding value obtained here (determined via polynomial fit) runs from 6.7 % at $T = 340$ K to 24.6 % at $T = 320$ K.

AQiso03 was investigated by Tamura and Shinoda with a flow-type apparatus. They determined three isotherms (at (323.15, 353.15, and 383.15) K) in a pressure range between (10 and 25) MPa.[36] Again, our solubility values for AQiso03 are mainly lower. To illustrate it, at $T = 320$ K, our s at $p =$ (10 and 15) MPa amounts to $(14.7 \cdot 10^{-6}$ and $307.3 \cdot 10^{-6})$ mol·dm^{-3}, compared to $(10.2 \cdot 10^{-6}$ and $470.0 \cdot 10^{-6})$ mol·dm^{-3} at $T = 323.15$ K, respectively (cf. also Figures S3a and S3b in the Supporting Information).[36]

In their study on both the solubility and the adsorption behavior of disperse dyestuffs, Tabata et al. reported solubility data of AQ04 in CO_2 for temperatures between (323.15 and 418.15) K and pressures up to about 23 MPa with a dynamic apparatus.[37] Since the solubility data are displayed in diagrams only, we had to resort to the numerical values from the reference data manual again.[32] Their data at $T = 323.15$ K coincide with the 320 K isotherm from Wagner's thesis[18] quite well, so that their results for identical temperatures are supposed to be somewhat lower. If we compare the isotherms measured by Wagner to those measured by Kautz at the same temperatures, there is no difference in the course of the isotherms, but Kautz obtained higher values above about 15 MPa.[17,18] Additionally, the old data from the static analytical method largely match Kautz's data; that data set, however, is limited to lower AQ04 equilibrium concentrations for instrument-based reasons.[5] At $p = 10$ MPa, the difference between the solubilities measured by Kautz and by Wagner is + 13.4 % for $T = 310$ K and + 20.5 % for $T = 320$ K, respectively. At $p = 15$ MPa, the difference amounts to + 19.0 % for $T = 310$ K, + 16.8 % for $T = 320$ K, + 9.9 % for $T = 330$ K, and + 2.2 % for $T = 340$ K, and the difference between the solubility measured by Kautz and by the static analytical method is + 2.6 % for $T = 340$ K. The additional data again are provided in the Supporting Information.

Ultimately, two different chromatographic carrier materials were employed for the experiments with AQ08 which resulted in almost identical results at all experimental conditions. The corresponding data from the static analytical method showed the same systematic shift to higher solubilities.[5] A respective diagram (Figure S6) is placed in the Supporting Information. For this substance, however, a sample was purified according to the initially described procedure and investigated in both the static and the flow apparatus at the same temperature $T = 310.1$ K for comparison.[7] The results were identical, and these findings were discussed in the paper by Wagner et al.[24]

From the results, it is evident that primarily the experimental conditions, i.e., the individual setup that governs how the equilibrium solubility is achieved and the purity of the employed sample, affect the data quality. The results from the cross-check experiments with AQ08 corroborated our notion. Thus, we consider the errors associated with the experimental parameters T, p, ρ, etc. subordinate on the outcome for the solubility. The fact that in three studies, i.e., Joung and Yoo on AQ01,[34] Gordillo et al. on AQ01,[35] and Tamura and Shinoda on AQiso03,[36] commercial samples were directly used (Tabata et al., however, purified their AQ04 sample by recrystallization from benzene[37]) could be a possible reason for the deviation to our results.

Modeling. There are two major concepts for modeling solubilities in supercritical fluids, equation of state (EoS) modeling and empirical density-based correlations. The EoS modeling usually requires not only selecting the most appropriate equation and mixing rule but also knowledge of pure component parameters of the solute. If those pure component parameters, for whatever reason, cannot be determined directly, their physical meaning gets lost, and such a parameter then is transformed into a fittable numerical value. Thus, solubility modeling by EoS is a challenging task. Already in 1986, Haselow et al. published a review on the performance of various equations of state on solubility of solids in supercritical fluids with a particular view on the question which equation qualifies best according to the characteristics of the system to be applied.[38] On the other hand, the (fully) empirical models work without additional solute properties. The so-called "density-based" concepts are developed from the observation that there is a linear relationship between the logarithm of the solubility s and the logarithm of the solvent density ρ (or the solvent density ρ) within a certain range of pressures and temperatures, but with particular emphasis on the latter statement. The density-based models are quite popular in chemical engineering because they are often very successful in correlating existing solubility data. Furthermore, these models give good results for a solvent density region (from 10 MPa to approximately 30 MPa), where not only technical SFC processes usually operate but also most solubility data are collected. In that region, the double logarithmic plot yields a linear function. Such a correlation is bound to fail for more extreme density regimes, e.g., when the solvent density becomes liquid-like ($\rho = 1000$ g·dm^{-3} and more) under the experimental conditions. Consequently, modeling or predictive extrapolation of solubility using such a model will be possible as long these limits are respected. It means that border regions, like low (subcritical) temperatures or very high pressures that are accompanied by liquid-like densities, as well as very low densities which, for example, occur at low pressures for the corresponding temperature, are unsuited for density-based concepts.

We performed solubility investigations in those regions as well, where we employed the static analytical method[4−8,10−13,30]

Table 8. Survey of the Model Parameters, the Derived Thermodynamic Properties, and the Average Relative Deviation for the Systems Presented Here Including AQ03 + CO_2[15]

model	AQ01	AQ02	AQ03	AQiso03	AQ04	AQ05	AQ08
				Chrastil, eq 8 [19]			
a	−5792.0	−6244.2	−6378.4	−6244.2	−7247.5,[a] −7990.4[b]	−7037.2	−9154.8,[b] −9799.9[c]
b	−30.316	−30.117	−29.503	−27.544	−28.578,[a] −32.034[b]	−33.000	−35.624,[b] −38.390[c]
k	6.588	6.799	7.101	6.794	7.378,[a] 8.277[b]	7.990	9.299,[b] 10.025[c]
100 ($\Delta s/s$)	3.4	4.2	5.4	4.0	3.8,[a] 5.6[b]	3.9	7.4,[b] 7.5[c]
ΔH/(kJ·mol^{-1})	48.16	51.92	53.03	51.92	60.26,[a] 66.44[b]	58.51	76.12,[b] 81.48[c]
				Sung and Shim, eq 9 [20]			
A	−27.947	−26.452	−30.724	−31.537	−28.219,[a] −19.554[b]	−22.120	−23.105,[b] −21.150[c]
B	−7181.2	−8106.4	−6641.3	−5447.9	−8034.3,[a] −12707.3[b]	−11223.3	−14060.8,[b] −16204.6[c]
C	4.9603	4.9631	5.9939	5.9989	6.0029,[a] 5.0113[b]	4.9932	6.0109,[b] 6.0034[c]
D	209.14	279.60	36.778	−89.775	121.37,[a] 733.90[b]	640.84	754.11,[b] 986.81[c]
100 ($\Delta y/y$)	3.2	3.8	5.4	4.2	3.8,[a] 5.0[b]	4.5	8.0,[b] 8.3[c]
				Clifford and co-workers, eq 10 [21]			
a	18.509	19.967	21.099	20.428	23.765,[a] 26.479[b]	24.637	30.706,[b] 32.177[c]
b	−8712.9	−9161.8	−8858.5	−8527.4	−9728.1,[a] −10552.2[b]	−9962.5	−12187.2,[b] −12672.1[c]
C/(m^3·kg^{-1})	0.0116	0.0121	0.0124	0.0118	0.0127,[a] 0.0145[b]	0.0139	0.0168,[b] 0.0175[c]
100 ($\Delta y/y$)	4.7	6.0	11.1	9.7	8.6,[a] 9.5[b]	10.3	14.1,[b] 15.8[c]
$\Delta_{sub}H$/(kJ·mol^{-1})	72.44,150.3 [41]	76.18	73.65	70.90	80.88,[a] 87.74[b]	82.83	101.33,[b] 105.36[c]
				del Valle and Aguilera, eq 11 [22,39]			
n	−5794.5	−6258.6	−6258.6	−6258.6	−7243.0,[a] −7990.2[b]	−7039.6	−9155.0,[b] −9800.6[c]
n'	−35.788	−38.671	−38.671	−38.671	−44.791,[a] −49.414[b]	−52.919	−12.507,[b] −60.779[c]
b	−30.313	−30.120	−29.606	−27.525	−28.575,[a] −32.029[b]	−32.997	−35.621,[b] −38.396[c]
k	6.5890	6.8061	7.0591	6.7982	7.3760,[a] 8.2762[b]	7.9910	9.2982,[b] 10.0258[c]
100 ($\Delta s/s$)	3.4	4.2	5.6	4.0	3.8,[a] 5.6[b]	3.9	7.4,[b] 7.2[c]
				Méndez-Santiago and Teja, eq 12 [23]			
A'	−11392.9	−12034.5	−11530.1	−11036.4	−12306.6,[a] −13451.5[b]	−13056.3	−16009.8,[b] −16697.5[c]
B'	3.7507	3.9751	4.0397	3.8288	4.0864,[a] 4.6891[b]	4.4792	5.5427,[b] 5.7837[c]
C'	18.626	20.180	20.554	19.840	22.822,[a] 25.241[b]	24.419	30.452,[b] 32.020[c]
100 ($\Delta y/y$)	6.3	8.9	14.7	13.2	12.9,[a] 12.8[b]	15.9	19.3,[b] 21.0[c]

[a] Filled directly into the extraction column; cf. Wagner's thesis.[18] [b] Precipitated on silanized kieselguhr; cf. Kautz's thesis.[17] [c] Precipitated on Chromosorb G-AW; cf. Kautz's thesis.[17]

and discussed the problem of proper modeling in a joint paper with theoreticians from the University at Cologne.[16]

The entire experimental conditions of the investigations described here, however, allow for density-based correlations. We tested and evaluated five different proposals, the three-parameter equation suggested by Chrastil,[19] the model by Sung and Shim, where a fourth parameter was introduced,[20] the three-parameter equation developed by Clifford and co-workers,[21] a four-parameter extension of Chrastil's model suggested by del Valle and Aguilera[22] and applied by Gómez-Prieto et al. to correlate solubilities of carotenes,[39] and ultimately the three-parameter equation developed by Méndez-Santiago and Teja.[23]

Chrastil's equation is

$$\ln\left(\frac{s}{s^0}\right) = \frac{a}{(T/\mathrm{K})} + b + k\ln\left(\frac{\rho}{\rho^0}\right) \tag{8}$$

where solubility s^0 and density $\rho^0 = 1$ g·dm^{-3}; and a, b, and k are the model constants, where k is an association number that represents the number of CO_2 molecules in an assumed solute−solvent complex. T stands for the absolute temperature. As parameter a depends on vaporization and solvation enthalpies of the solute, Chrastil suggested the relation $a = (\Delta H/R)$, in which ΔH was called "total reaction heat".[19] R is the universal gas constant.

Sung and Shim added an additional parameter. The resulting equation is

$$\ln y = A + \frac{B}{(T/\mathrm{K})} + \left(C + \frac{D}{(T/\mathrm{K})}\right)\ln\left(\frac{\rho}{\rho^0}\right) \tag{9}$$

where y is the saturation mole fraction of the solute; ρ is the solvent density; and A, B, C, and D are adjustable parameters.[20]

The next model proposed by Clifford and co-workers correlates the solubility via

$$\ln\left(\frac{yp}{p_{\mathrm{ref}}}\right) = a + \frac{b}{(T/\mathrm{K})} + C(\rho - \rho_{\mathrm{ref}}) \tag{10}$$

Here, y again is the mole fraction solubility; p is the pressure; and a, b, and C are the model parameters. p_{ref} denotes the standard pressure $p_{\mathrm{ref}} = 0.1$ MPa, and ρ_{ref} is a reference density which was set at $\rho_{\mathrm{ref}} = 700$ g·dm^{-3} by the authors.[21] Upon a suggestion by Miller et al., the parameter b can approximately be related to the sublimation enthalpy of the solid $\Delta_{sub}H$ by $\Delta_{sub}H = -Rb$.[40]

The following equation by del Valle and Aguilera was taken from a later paper[39]

$$\ln\left(\frac{s}{s^0}\right) = \frac{n}{(T/\mathrm{K})} + \frac{n'}{(T/\mathrm{K})^2} + b + k\ln\left(\frac{\rho}{\rho^0}\right) \tag{11}$$

where s/s^0 and ρ/ρ^0 are the model variables and n, n', b, and k are the respective constants.[22]

The last density-based correlation that was applied to our data is the equation developed by Méndez-Santiago and Teja

$$\ln\left(y\frac{p}{p^0}\right) = \frac{A'}{(T/\mathrm{K})} + \frac{B'}{(T/\mathrm{K})}\frac{\rho}{\rho^0} + C' \tag{12}$$

The solubility again is introduced as mole fraction y, and A', B', and C' are the adjustable parameters.[23] Like in the model proposed by Clifford and co-workers, the pressure p/p^0 ($p^0 = 0.1$ MPa) is incorporated.

The optimum parameters for each model are determined in the same way via minimization of the following objective function F

$$F = \sum_{i=1}^{N_D} \left(\frac{(Z^{exptl} - Z^{calcd})}{Z^{exptl}} \right)^2 \text{ with } Z = s \text{ or } y \qquad (13)$$

where N_D is the number of experimental data. To evaluate the quality of the correlation, the average relative deviation is determined according to

$$\frac{\Delta Z}{Z} = \frac{1}{N_D} \sum_{i=1}^{N_D} \left| \frac{(Z^{exptl} - Z^{calcd})}{Z^{exptl}} \right| \text{ with } Z = s \text{ or } y \qquad (14)$$

Table 8 lists the optimum parameters together with the derived thermodynamic properties and the determined average relative deviation for each system presented in this work including AQ03 + CO_2 that was not subject to correlation in the 1999 paper.[15] A comparison between experimental data and calculation for each individual data point can easily be done by employing the given equations and the associated parameters.

The astonishing finding is that the introduction of a fourth parameter does not significantly improve the correlation. Moreover, the performance seems to deteriorate when the pressure is included. The average relative deviation $\Delta y/y$ for the correlations according to Clifford and co-workers as well Méndez-Santiago and Teja is usually higher than 5 %, partly outreaching even 10 %.[21,23] Chrastil's model and the one-parameter extension from del Valle and Aguilera performed best,[19,22,39] so that Chrastil's simple three-parameter concept deservedly remains a good tool, and thus it has frequently occurred in the literature since its publication in 1982. Anyway, the derived enthalpic properties shall not be accepted unconditionally, but at most as a rough estimation. For example, the experimentally obtained literature value for the sublimation enthalpy of AQ01, $\Delta_{sub}H(\text{AQ01}) = 150.3\ \text{kJ}\cdot\text{mol}^{-1}$,[41] is more than twice the value from the correlation.[21] The "total reaction heat" ΔH according to Chrastil is something different[19] and was discussed in an earlier paper.[31]

Conclusions

The solubility of a series of six anthraquinone disperse dyestuffs has been investigated between (299 and 346) K and pressures up to maximum 20 MPa, and five fully empirical correlations have been examined including an additional seventh member of that series.

Our particular setup for solubility experiments requires a separate calibration, where "normal" liquid (organic) solvents have to be used. Apart from the calibration, the experimental setup, the sample characteristics, and how the operations are carried out have a bigger impact on data accuracy than, for example, the precision and accuracy of the measuring instruments. So, a proper selection of calibration solvents is the first step toward precise and correct results. That was further endorsed by comparison of our data both with literature values and our own results but obtained by a different method.

Looking at the empirical density-based correlation concepts, which were randomly selected, leads to an astonishing finding. Provided that the basic requirements for the model validity are fulfilled (i.e., primarily to keep experimental conditions within a certain density domain, which our investigations met; of course, always provided that data scattering is limited and the number of values is not too limited, either), a simple model like, e.g., Chrastil's three-parameter approach[19] performs very well, and additional (adjustable) parameters do not automatically result in a better correlation.

Supporting Information Available:

The calibration functions to calculate the solubility from the recorded VIS spectrum, the illustration of a calibration function, and the comparison of our results with literature data where available (AQ01, AQiso03, AQ04, and AQ08). This material is available free of charge via the Internet at http://pubs.acs.org.

Literature Cited

(1) Santos, W. L. F.; Moura, A. P.; Povh, N. P.; Muniz, E. C.; Rubira, A. F. Anthraquinone and azo dyes in dyeing processes of PET films and PET knitted fabrics using supercritical CO_2 medium. *Macromol. Symp.* **2005**, *229*, 150–159.

(2) Park, M.-W.; Bae, H.-K. Dye distribution in supercritical dyeing with carbon dioxide. *J. Supercrit. Fluids* **2002**, *22*, 65–73.

(3) Hendrix, W. A. Progress in supercritical CO_2 dyeing. *J. Ind. Textiles* **2001**, *31*, 43–56.

(4) Haarhaus, U.; Swidersky, P.; Schneider, G. M. High-pressure investigations on the solubility of dispersion dyestuffs in supercritical gases by VIS/NIR-spectroscopy. Part I−1,4-Bis-(octadecylamino)-9,10-anthraquinone and Disperse Orange 13 in CO_2 and N_2O up to 180 MPa. *J. Supercrit. Fluids* **1995**, *8*, 100–106.

(5) Swidersky, P.; Tuma, D.; Schneider, G. M. High-pressure investigations on the solubility of anthraquinone dyestuffs in supercritical gases by VIS-spectroscopy. Part II−1,4-Bis-(*n*-alkylamino)-9,10-anthraquinones and Disperse Red 11 in CO_2, N_2O, and CHF_3 up to 180 MPa. *J. Supercrit. Fluids* **1996**, *9*, 12–18.

(6) Schneider, G. M.; Kautz, C. B.; Tuma, D. High-pressure investigations on the solubility of synthetic and natural dyestuffs in supercritical gases by VIS-spectroscopy up to 180 MPa. In *High Pressure Chemical Engineering. Process Technology Proceedings 12*; Rudolf von Rohr, Ph., Trepp, C., Eds.; Elsevier: Amsterdam, 1996; pp 259−264.

(7) Tuma, D.; Schneider, G. M. High-pressure solubility of disperse dyes in near- and supercritical fluids: measurements up to 100 MPa by a static method. *J. Supercrit. Fluids* **1998**, *13*, 37–42.

(8) Tuma, D.; Schneider, G. M. Determination of the solubilities of dyestuffs in near- and supercritical fluids by a static method up to 180 MPa. *Fluid Phase Equilib.* **1999**, *158−160*, 743–757.

(9) Tuma, D.; Wagner, B.; Schneider, G. M. Comparative solubility investigations of anthraquinone disperse dyes in near- and supercritical fluids. *Fluid Phase Equilib.* **2001**, *182*, 133–143.

(10) Kraska, T.; Leonhard, K. O.; Tuma, D.; Schneider, G. M. Correlation of the solubility of low-volatile organic compounds in near- and supercritical fluids. Part I: applications to adamantane and β-carotene. *J. Supercrit. Fluids* **2002**, *23*, 209–224.

(11) Kraska, T.; Jurtzik, J.; Tuma, D.; Schneider, G. M. Correlation of the solubility of low-volatile organic compounds in near- and supercritical fluids. *Russ. J. Phys. Chem.* **2003**, *77*, S51−S57.

(12) Tuma, D.; Wagner, B.; Schneider, G. M. High-pressure solubility measurement of solids in near- and supercritical fluids. In *Supercritical Fluids as Solvents and Reaction Media*; Brunner, G., Ed.; Elsevier: Amsterdam, San Diego, Oxford, London, 2004; pp 121−146.

(13) Kraska, T.; Tuma, D. High-pressure phase equilibria in binary and ternary mixtures with one near- or supercritical and one high-molecular component. New insights for application and theory. *J. Mater. Sci.* **2006**, *41*, 1547–1556.

(14) Kautz, C. B.; Wagner, B.; Schneider, G. M. High-pressure solubility of 1,4-bis-(n-alkylamino)-9,10-anthraquinones in near- and supercritical carbon dioxide. *J. Supercrit. Fluids* **1998**, *13*, 43–47.

(15) Wagner, B.; Kautz, C. B.; Schneider, G. M. Investigations on the solubility of anthraquinone dyes in supercritical carbon dioxide by a flow method. *Fluid Phase Equilib.* **1999**, *158−160*, 707–712.

(16) Kraska, T.; Leonhard, K. O.; Tuma, D.; Schneider, G. M. Correlation of the solubility of low-volatile organic compounds in near- and supercritical fluids. Part II. Applications to Disperse Red 60 and two disubstituted anthraquinones. *Fluid Phase Equilib.* **2002**, *194−197*, 469–482.

(17) Kautz, C. B. Fluidchromatographische Untersuchungen (SFC) an organischen Substanzen mit überkritischem Kohlendioxid: Bestimmung der Kapazitätsverhältnisse von Polyphenylen und substituierten Benzolderivaten sowie spektroskopische Löslichkeitsuntersuchungen an Anthrachinonfarbstoffen bis 20 MPa. Doctoral Thesis (ScD), University of Bochum, 1996; Cuvillier: Göttingen, 1997.

(18) Wagner, B. Untersuchungen zur Löslichkeit von Anthrachinonfarbstoffen in nah- und überkritischem Kohlendioxid mit einer Strömungsmethode bis 20 MPa. Doctoral Thesis (ScD), University of Bochum, 1998.

(19) Chrastil, J. Solubility of solids and liquids in supercritical gases. *J. Phys. Chem.* **1982**, *86*, 3016–3021.

(20) Sung, H.-D.; Shim, J.-J. Solubility of C. I. Disperse Red 60 and C. I. Disperse Blue 60 in supercritical carbon dioxide. *J. Chem. Eng. Data* **1999**, *44*, 985–989.

(21) Safa Özcan, A.; Clifford, A. A.; Bartle, K. D.; Lewis, D. M. Solubility of disperse dyes in supercritical carbon dioxide. *J. Chem. Eng. Data* **1997**, *42*, 590–592.

(22) del Valle, J. M.; Aguilera, J. M. An improved equation for predicting the solubility of vegetable oils in supercritical CO_2. *Ind. Eng. Chem. Res.* **1988**, *27*, 1551–1553.
(23) Méndez-Santiago, J.; Teja, A. S. The solubility of solids in supercritical fluids. *Fluid Phase Equilib.* **1999**, *158*−*160*, 501–510.
(24) Wagner, B.; Nishioka, M.; Tuma, D.; Maiwald, M.; Schneider, G. M. Sample purification for spectroscopic high-pressure investigations by dynamic supercritical fluid extraction. *J. Supercrit. Fluids* **1999**, *16*, 157–165.
(25) Maiwald, M. Solvatochromie in überkritischen Fluiden. Doctoral Thesis (ScD), University of Bochum, 1997; Cuvillier: Göttingen, 1997.
(26) Span, R.; Wagner, W. A new equation of state for carbon dioxide covering the fluid region from the triple-point temperature to 1100 K at pressures up to 800 MPa. *J. Phys. Chem. Ref. Data* **1996**, *25*, 1509–1596.
(27) Wagner, W.; Overhoff, U. *ThermoFluids Version 1.0 (Build 1.0.0)*; Springer: Berlin, 2006.
(28) Hammam, H.; Sivik, B. Phase behavior of some pure lipids in supercritical carbon dioxide. *J. Supercrit. Fluids* **1993**, *6*, 223–227.
(29) Dohrn, R.; Bertakis, E.; Behrend, O.; Voutsas, E.; Tassios, D. Melting point depression by using supercritical CO_2 for novel melt dispersion micronization process. *J. Mol. Liq.* **2007**, *131*−*132*, 53–59.
(30) Haarhaus, U. Spektroskopische Hochdruckuntersuchungen zur Löslichkeitsbestimmung von Dispersionsfarbstoffen in überkritischen Gasen bei Drücken bis zu 2 kbar und Temperaturen zwischen 300 und 410 K. Doctoral Thesis (ScD), University of Bochum, 1992; Shaker: Aachen, 1992.
(31) Tuma, D.; Wagner, B.; Schneider, G. M. Temperature, pressure and density dependencies of the solubilities of low-volatility organic compounds in compressed gases. Part 1. Solution energies from solubility data for disperse dyestuffs up to 20 MPa. *Phys. Chem. Chem. Phys.* **2002**, *4*, 968–973.
(32) Gupta, R. B.; Shim, J.-J. *Solubility in Supercritical Carbon Dioxide*; CRC Press: Boca Raton, London, New York, 2007.
(33) Chimowitz, E. H.; Pennisi, K. J. Process synthesis concepts for supercritical gas extraction in the crossover region. *AIChE J.* **1986**, *32*, 1665–1676.
(34) Joung, S. N.; Yoo, K.-P. Solubility of disperse anthraquinone and azo dyes in supercritical carbon dioxide at 313.15 to 393.15 K and from 10 to 25 MPa. *J. Chem. Eng. Data* **1998**, *43*, 9–12.
(35) Gordillo, M. D.; Pereyra, C.; Martínez de la Ossa, E. J. Measurement and correlation of solubility of Disperse Blue 14 in supercritical carbon dioxide. *J. Supercrit. Fluids* **2003**, *27*, 31–37.
(36) Tamura, K.; Shinoda, T. Binary and ternary solubilities of disperse dyes and their blend in supercritical carbon dioxide. *Fluid Phase Equilib.* **2004**, *219*, 25–32.
(37) Tabata, I.; Lyu, J.; Cho, S.; Tominaga, T.; Hori, T. Relationship between the solubility of disperse dyes and the equilibrium dye adsorption in supercritical fluid dyeing. *Color Technol.* **2001**, *117*, 346–351.
(38) Haselow, J. S.; Han, S. J.; Greenkorn, R. A.; Chao, K. C. Equation of state for supercritical extraction. In *Equations of State. Theories and Applications. ACS Symp. Ser. 300*; Chao, K. C., Robinson, R. L., Eds.; American Chemical Society: Washington DC, 1986; pp 156−178.
(39) Gómez-Prieto, M. S.; Caja, M. M.; Santa-María, G. Solubility in supercritical carbon dioxide of the predominant carotenes of tomato skin. *J. Am. Oil Chem. Soc.* **2002**, *79*, 897–902.
(40) Miller, D. J.; Hawthorne, S. B.; Clifford, A. A.; Zhu, S. Solubility of polycyclic aromatic hydrocarbons in supercritical carbon dioxide from 313 to 523 K and pressures from 100 to 450 bar. *J. Chem. Eng. Data* **1996**, *41*, 779–786.
(41) Datye, K. V.; Kangle, P. J.; Milićević, B. Experimentelle Beiträge zur Phänomenologie der Färbung von Polyestersubstraten mit Dispersionsfarbstoffen bei Temperaturen von 200 °C. *Textilveredlung* **1967**, *2*, 263–274.

Received for review April 11, 2008. Accepted July 9, 2008. Financial support of this investigation by the Fonds der Chemischen Industrie e. V. is gratefully acknowledged.

JE800252Z